2

3

10

11

12

13

14

15

16

17

18

19

20

21

22

23

24

27

28

29

30

31

32

33

34

35

36

37

38

39

Magnetic Relaxation Seen in a Rapidly Evolving Light Bridge in a Sunspot

Donguk Song D,^{1,2} Eun-Kyung Lim D,¹ Jongchul Chae D,³ Yeon-Han Kim D,¹ Yukio Katsukawa D,² and Vasyl Yurchyshyn D⁴

¹Korea Astronomy and Space Science Institute, 776 Daedeok-daero, Yuseong-gu, Daejeon 34055, Republic of Korea
²National Astronomical Observatory of Japan, 2-21-1 Osawa, Mitaka, Tokyo 181-8588, Japan
³Astronomy Program, Department of Physics and Astronomy, Seoul National University, Gwanak-gu, Seoul 08826, Republic of Korea
⁴Big Bear Solar Observatory, New Jersey Institute of Technology, Big Bear City, CA 92314, USA

ABSTRACT

We report a magnetic relaxation process inside a sunspot associated with the evolution of a transient LB. Taking advantage of high-resolution imaging and spectropolarimetric data taken by the 1.6-meter Goode Solar Telescope at Big Bear Solar Observatory, we observed the evolutionary process of a rapidly evolving LB. The LB was formed as a result of the strong intrusion of penumbral filaments with relatively horizontal fields into the vertical umbral field region. As the LB developed, the magnetic non-potentiality inside the sunspot increases, and tangential discontinuity of the magnetic field appeared, especially around the local region where the magnetic field topology changes rapidly. Indeed, we detected strong current density at this region. Bright jets, which are intermittently and recurrently observed in the chromosphere, dissipate the magnetic energy of the sunspot through magnetic reconnection occurring along this strong current region. Thereafter, no additional horizontal magnetic field was supplied into the LB, and the LB magnetic fields continuously changed into vertical magnetic fields. This process of horizontal field weakened the LB fields and broke the balance between LB fields and surrounding umbral fields, causing the LB to fragment and turn into umbral dots. Our findings provide a comprehensive perspective not only on the evolution of an LB itself, but also on its impacts in the neighboring regions, including the chromospheric activity and the change of magnetic energy of a sunspot.

Keywords: sunspots - Sun: chromosphere - Sun: magnetic fields - magnetic reconnection

1. INTRODUCTION

A light bridge (LB) is one of the substructures frequently observed in a sunspot, appearing relatively bright compared to a surrounding dark umbra (Muller 1979; Sobotka et al. 1994). An LB mainly manifests as an elongated structure that crosses a sunspot umbra, and while it has the same magnetic polarity as the host sunspot, its magnetic field structure is significantly different. The typical magnetic field structure above an LB is known as a canopy structure, that has the field-free plasma region or weak magnetic fields in the photosphere (Leka 1997; Schüssler & Vögler 2006; Jurčák et al. 2006). Furthermore, the presence of a strong horizontal magnetic field along the LB is frequently observed (Okamoto & Sakurai 2018), which is a distinct feature from the magnetic field structure of the host sunspot umbra. The magnetic field structure of the LB becomes an important factor in determining its internal morphology: a filamentary LB showing bundles of filaments with a relatively enhanced horizontal magnetic field inside the LB (Louis et al. 2008; Lim et al. 2020) and a granular LB composed of convective cells similar to the granules seen in the quiet Sun (Lagg et al. 2014; Song et al. 2017a).

The formation of an LB may cause significant inhomogeneity in the magnetic field structure of a sunspot, which may lead to changes in the internal structure and magnetic energy inside a sunspot. Previous high-resolution obser-

Corresponding author: Donguk Song

donguksong@kasi.re.kr

vational and theoretical studies have suggested that the LB formation may be caused by the intrusion of penumbral filaments (Katsukawa et al. 2007) and the emergence of horizontal magnetic fields inside an umbra (Toriumi et al. 2015). This LB formation process may gradually increase the tangential discontinuity of the magnetic field inside a sunspot (Song et al. 2015), leading to the sunspot activity and changes in the solar atmosphere. Fine-scale plasma ejections (Shimizu et al. 2009; Louis et al. 2014; Song et al. 2017a; Zhang et al. 2017; Tian et al. 2018; Yang et al. 2019a; Lim et al. 2020) and enhanced brightening (Berger & Berdyugina 2003; Song et al. 2017b) are one of the representative solar atmospheric phenomena related to the LB activity.

These chromospheric phenomena are observational evidences for the vigorous interaction that occur between the different magnetic field structures of a sunspot and an LB, such as magnetic reconnection (Shimizu et al. 2009; Louis et al. 2015; Bharti et al. 2017; Yang et al. 2019b). Bharti et al. (2017) have for the first time reported a manifestation of successive magnetic reconnection seen above a penumbral filament digging into a sunspot umbra, and suggested that magnetic reconnection may occur between curved flux rope-like fields in the lower part of the penumbral intrusion and vertical umbral fields. Louis et al. (2015) and Yang et al. (2019b) found an observational evidence of a small-scale magnetic flux emergence observed in the strong magnetised environment, such as an LB, and reported that it was associated with the transient brightening and plasma ejections in the chromosphere. These previous results suggest that the LB formation and evolution make a significant contribution to chromospheric activity of a sunspot and internal magnetic field energy changes.

The lifetime of an LB is typically several days. During this period, an LB undergoes a variety of physical changes that directly impact the activity and evolution of a sunspot (Vazquez 1973). Shimizu (2011) reported a long-term evolution study on an LB, and demonstrated that the changes of the activity and phenomena appearing in the solar chromosphere are different depending on the internal magnetic structures and gas flows of the LB. Griñón-Marín et al. (2021) also reported through their study on the long-term evolution of three different LBs observed on the same sunspot that each LB has its own peculiarities with time, and that the atmospheric parameters may be changed accordingly.

Here we report our uninterrupted observations of an LB from birth to decay over the period of several hours. This rapidly evolving LB provided us with a nice chance of comprehensively studying the formation and decay of an LB with focus on the change of magnetic field configuration and the associated chromospheric activity. The paper is organized as follows. Observations and data analysis are described in Section 2. Section 3 present our results. Section 3.1 provides a full overview of the evolution of a LB in the photosphere. A description of temporal changes in the magnetic fields within the LB according to its evolutionary stage is given in the Section 3.2. Section 3.3 describes the chromospheric activity in sunspots following the LB evolution, i.e. the nature of the bright jets. Finally, in Section 4, our findings are summarized, and discuss about the entire process of the short-term evolution of an LB and the magnetic relaxation process of a sunspot observed during the LB formation and evolution.

2. OBSERVATIONS AND DATA ANALYSIS

We observed a leading sunspot in the NOAA 12080 active region located in the southern hemisphere (-515",-198") using the 1.6-meter Goode Solar Telescope (GST) installed at Big Bear Solar Observatory (BBSO) for about 2 hours from 16:34:00 UT on June 5, 2014. Our observations were performed simultaneously by using three different instruments installed in the Coudé room of BBSO with support of a high-order adaptive optics (AO; Cao et al. 2010) system: the Fast Imaging Solar Spectrograph (FISS; Chae et al. 2013), the Near Infra-Red Imaging Spectropolarimeter (NIRIS; Cao et al. 2012), and the TiO 705.7 nm broadband imager.

The FISS was designed as a dual-channel Echelle spectrograph, consisting of a field scanner, a single mirror used as a collimator and an imager, two bandpass filters, an Echelle grating with the blaze angle of 63.4° , and two CCD cameras. It can cover spectral windows in a wide range from visible to near-infrared light, but observes the solar chromosphere generally using two spectral bands simultaneously. Here, we carried out the high-resolution observations of the sunspot using the H α and Ca II 854.2 nm lines with the aid of a higher-order AO consisting of 308 sub-apertures (Shumko et al. 2014). The wavelength range covers from -0.53 nm to +0.45 nm with a spectral sampling of 19 mÅ in the H α line, and is from -0.70 nm to +0.61 nm with a spectral sampling of 26 mÅ in the Ca II 854.2 nm line. The spatial sampling of both lines is 0.''16, and the temporal cadence is about 22 seconds.

We measured linear and circular polarizations of the sunspot in the Fe I 1564.85 nm line using the NIRIS. The NIRIS was designed based on the dual Fabry-Pérot interferometer. Its spectral range is from 1564.69 nm to 1565.14 nm with a spectral sampling of 75.9 mÅ. The spatial sampling is about 0."16, and the temproal cadence is about

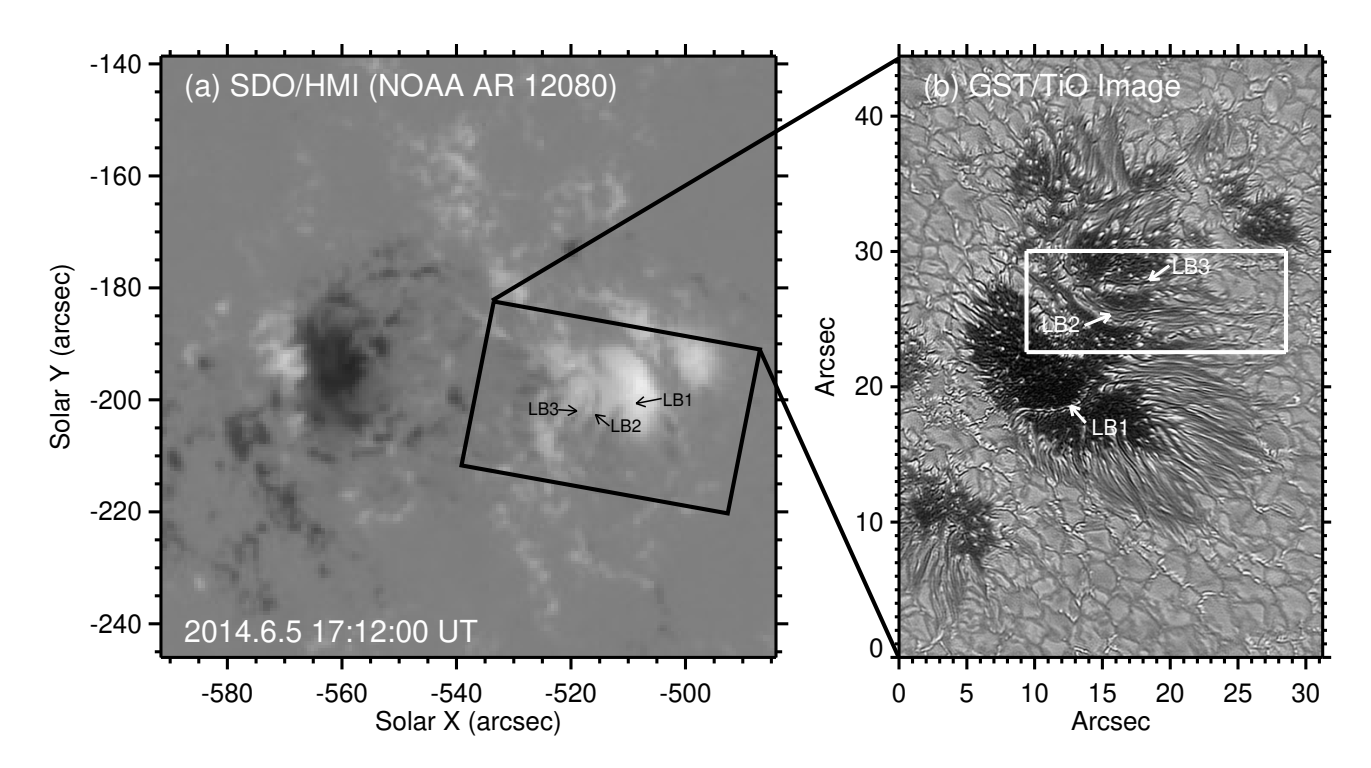


Figure 1. (a) SDO/HMI magnetogram of NOAA 12080 active region obtained on June 5, 2014 at 17:12:00 UT. The black rectangle box represents our observation region covering the field of view (FOV) of 31" × 44". (b) Photospheric image of an leading sunspot of NOAA AR 12080 taken by the broadband TiO 705.7 nm imager. Three LBs seen inside the suspot were indicated by "LB1", "LB2", and "LB3", respectively. The white box shows the FOV of the region of interest in which is the same as the FOV of the panel in Figure 2.

3 minutes. We inverted the Stokes profiles using the Milne-Eddington Stokes inversion code implemented by J. Chae (Landi Degl'Innocenti 1992; Lim et al. 2020), and solve the 180° ambiguity in the azimuth of the observed transverse magnetic fields (Moon et al. 2003). Finally, we obtained photospheric images using the broadband TiO 705.7 nm imager with a spatial sampling of about 0."0375 every 15 seconds.

Figure 1 (a) shows a line-of-sight (LOS) magnetogram of the NOAA 12080 active region obtained by the Helioseismic and Magnetic Imager (HMI; Schou et al. 2012) onboard the Solar Dynamics Observatory (SDO; Pesnell et al. 2012). This active region contains two large sunspots with opposite polarities (β -type based on the Mount Wilson classification; Hale et al. 1919) and several small pores in their vicinity. Our observation area, covering $31'' \times 44''$, is an entire region of a leading sunspot with a positive polarity, and is marked with a black box in the SDO/HMI magnetogram. Figure 1 (b) represents a photospheric image taken by the broadband TiO imager at 17:12:00 UT. This is a speckle reconstructed using the Kiepenheuer-Institut Speckle Interferometry Package code (Wöger et al. 2008). We find from the figure that the sunspot shows an asymmetrical shape that penumbral structures develop only in one direction of the sunspot umbra. It is divided into four cores by three different LBs: "LB1", "LB2", and "LB3" indicated in Figure 1. "LB2" is a main target of this study that lies long in the north-south direction and has filamentary structures inside.

3. RESULTS

3.1. Temporal Evolutions of a Light Bridge

A remarkable finding of this study is that the internal structure of an LB changes rapidly and distinctly in a short time. This is well shown in the sequential images of the TiO 705.7 nm band. As shown in Figure 2, the LB is observed in five different shapes depending on its evolutionary stage. The LB formation was first observed in the images taken by the SDO/HMI around 15:21:00 UT on June 5, 2014. One of the penumbral filament located at the end of the sunspot began to be rapidly penetrate into an umbral region, and, as a result, the LB, which we are interested in, formed along this filament.

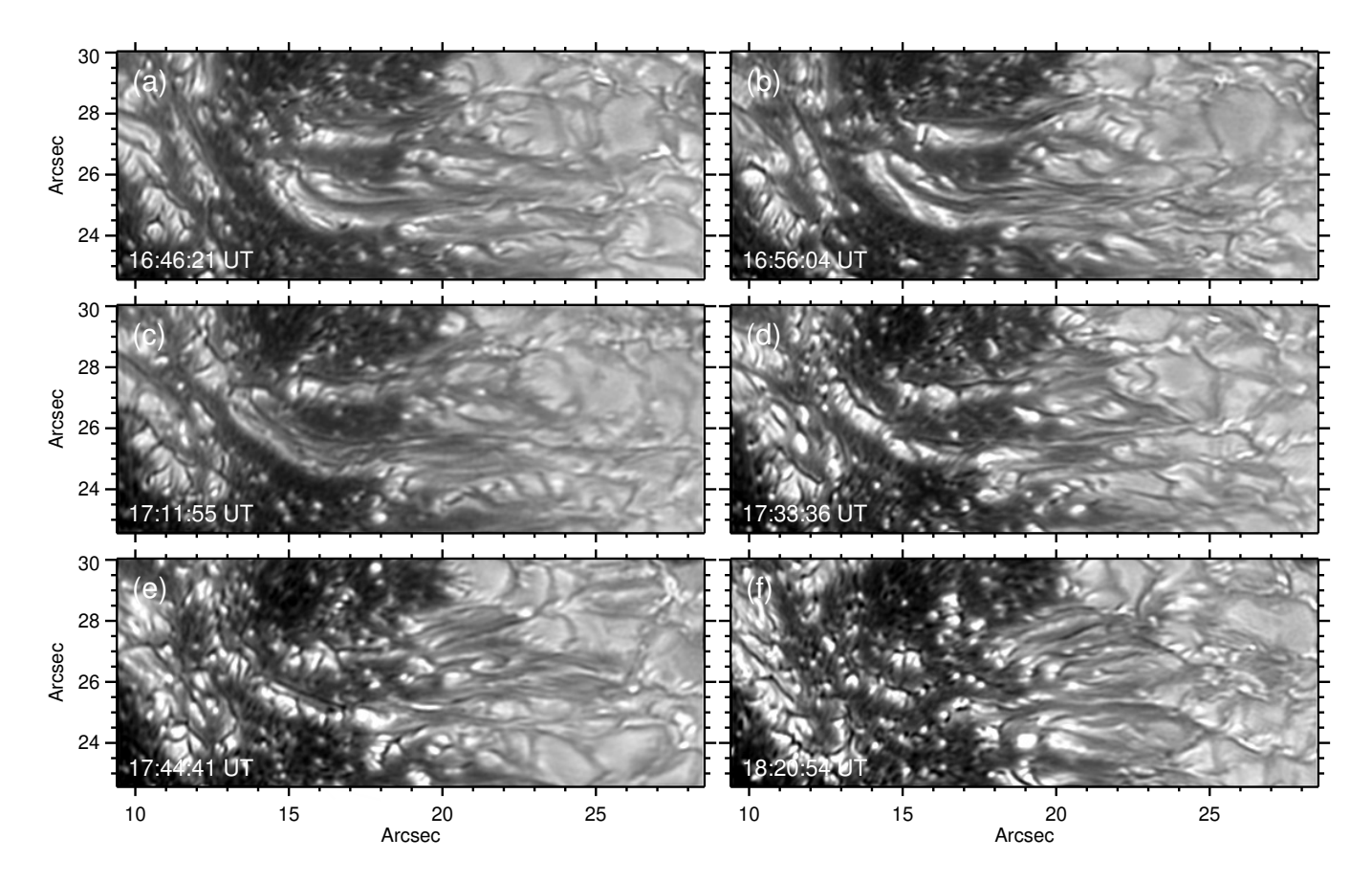


Figure 2. Temporal evolution of a LB in the photosphere. The FOV corresponds to the white box shown in Figure 1. (An animation of this figure is available.)

Our observations started at 16:39:02 UT, about an hour after the LB began to form, at which point the LB had already formed across more than half of the umbral region (Figure 2 (a)). After then, we can see that several penumbral filaments continuously penetrate into the developing LB (Figure 2 (b)). This leads to the formation of an elongated filament bundle in the umbra, approximately 1700 km in width along the LB. At 17:11:55 UT, the LB completely divided the sunspot umbra into two umbral cores, as a filamentary LB (Figure 2 (c)). Interestingly, at 17:33:36 UT, the filamentary structures located along the LB suddenly disappear and the shape of the LB changes into a chain of convective cells (Figure 2 (d) & (e)), i.e., it becomes a granular LB. In the latter part of our observations, the LB decayed gradually (Figure 2 (f)). Our data show in detail an evolutionary process of the LB from its development to decay with the high temporal and spatial resolutions.

Figure 3 (a) and (b) show transverse velocity fields determined by tracking 21 consecutive images of the TiO 705.7 nm band taken for 6 minutes from 3.4 and 27.6 minutes after the start of our observation, respectively. This was determined by applying a nonlinear affine velocity estimator (NAVE) developed by Chae & Sakurai (2008). We noted in the figure the early stages of the observation, especially the transverse velocity fields observed during the time when the LB is forming. The predominant flow observed along the LB is bidirectional flow, and the pattern of the transverse velocity fields is aligned well with the expansion direction of penumbral filaments penetrating into the umbra (Figure 3 (a)). The average transverse speed measured inside the LB is about 0.7 km s⁻¹, and the fast flows reaching up to 1.4 km s⁻¹ are distributed around both the ends of the penumbral filaments. In addition, in Figure 3 (b), we see filament bundles that are rapidly intruding into the interior of the formed LB. The corresponding transverse velocity fields are marked with red arrows. The measured speed of filament intrusion reaches up to 2.0 km s⁻¹, and their tips dig into the borders of the umbra positioned at both the lateral sides of the LB. As the filaments continue to penetrate inside the LB, we can see that the internal shape and magnetic field structure of the LB gradually evolve into a filamentary LB. The growth rate of the LB is approximately 0.48 km s⁻¹, which is slower than the maximum speed of filament

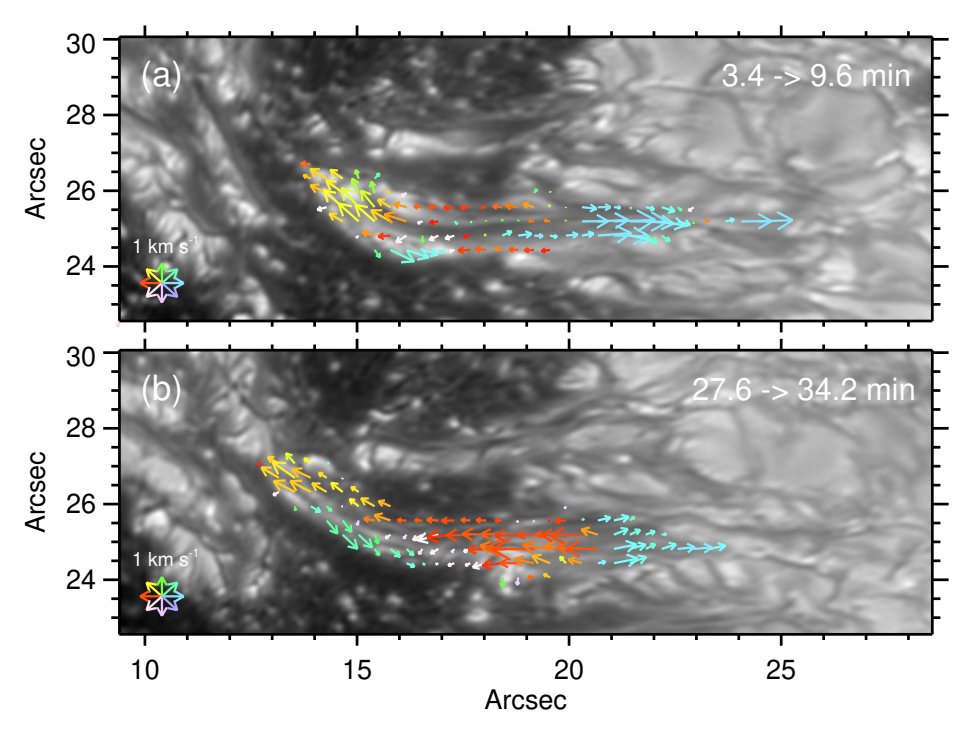


Figure 3. Transverse velocity fields in the internal structures of the LB determined by the NAVE method. They are determined by tracking 21 consecutive images of the TiO 705.7 nm band taken for 6 minutes from (a) 3.4 and (b) 27.6 minutes after the start of our observation (from 16:39:02 UT), respectively. The length and color of arrows indicates the speed and direction of the flow.

intrusion mentioned above, but find to be much faster than that of a typical LB formation previously reported by Katsukawa et al. (2007) and Griñón-Marín et al. (2021).

3.2. Evolutions of Magnetic Fields

It is expected that the shape changes inside the LB are closely related to the changes in the internal magnetic field structures of the LB depending on its evolutionary stage. Figure 4 shows maps of photospheric intensity (I/I_{QS}) , vertical magnetic field (B_z) , horizontal magnetic field (B_h) , and magnetic field inclination at the specific evolutionary stages of the LB of our interest. We normalized the intensity using the average intensity obtained around the quiet Sun (I_{QS}) , and corrected the projection effect in the vector magnetogram. We see from the B_z map that the vertical magnetic field strength of the LB is lower than that of the host sunspot umbra regardless of its morphology. This is consistent with the results of previous studies (Griñón-Marín et al. 2021). Here we note the change in the inclination of the magnetic field observed along the LB. In a series of inclination maps, we find that the magnetic field structure along the LB relatively becomes horizontal, and then returns to vertical fields again. This illustrates that the magnetic field structure within the sunspot undergoes rapid changes.

Figure 5 shows a more quantitative representation of the temporal changes in intensity and magnetic field structure described above. In the figure, the square symbols represent the average values of I/I_{QS} , B_z , B_h , and inclination, which were calculated using data from all pixels within the selected region outlined in red above the LB, as shown in Figure 4. Each error bar indicates the 1σ value for the spatial distribution of each physical quantity. One notable finding is the rapid increase and decrease in I/I_{QS} by more than 20% depending on the evolutionary stages of the LB. This variation is closely related to the change in the internal structures of the LB. Specifically, the photospheric intensity decreased rapidly during the formation of the LB and then increased again at the same time as the filamentary structures disappeared inside the LB. We see that the photosphere intensity was equal to the average intensity measured in the quiet Sun when the granular pattern appeared inside the LB afterwards, and finally the intensity gradually decreased again as the LB disappeared.

The second thing we noticed is that that inclination and B_z exhibit marked and rapid changes according to the evolutionary stages of the LB. In particular, we find from the plots that these changes can be divided into three parts

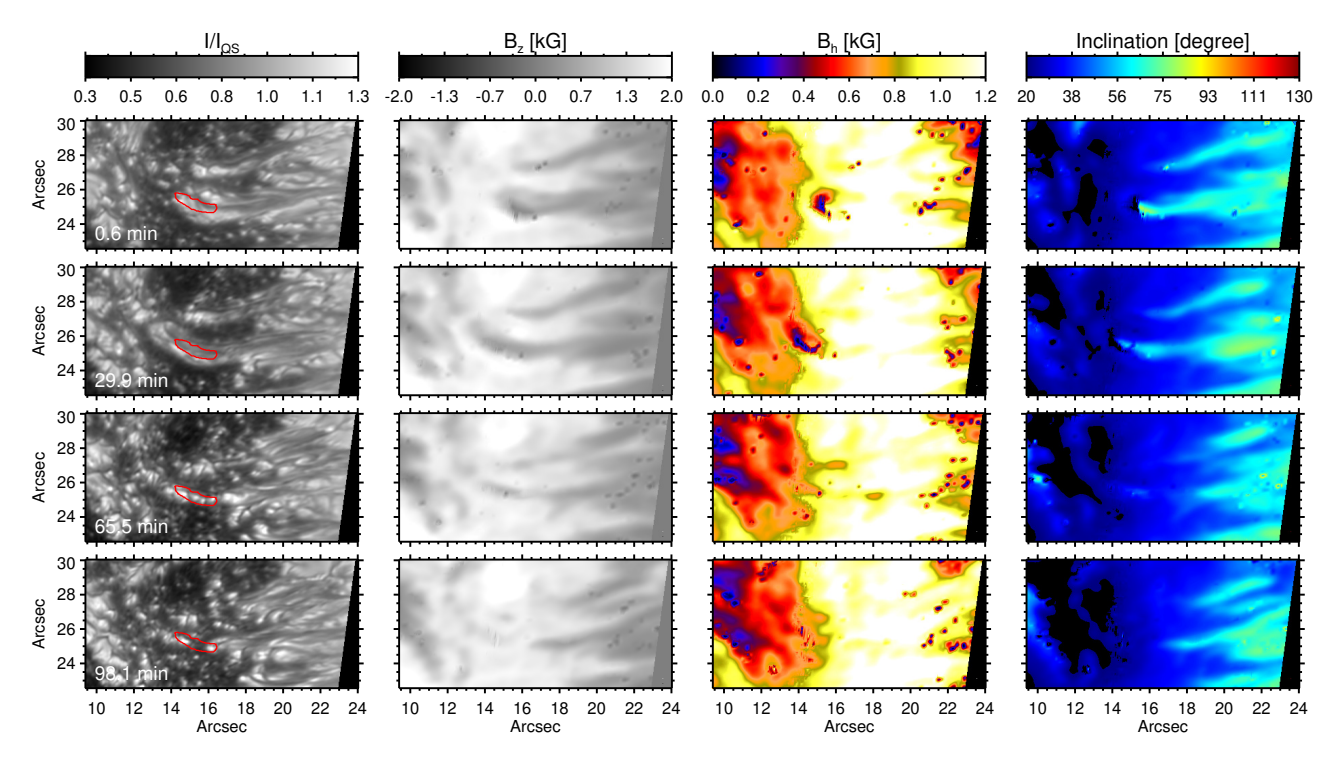


Figure 4. I/I_{QS} , B_z , B_h , and inclination maps (left to right) according to the evolutionary stage of the LB. Here, we set the observation time of 16:39:02 UT to t = 0 min. The red contour lines shown in the I/I_{QS} maps are the area we used to determine the temporal variations of physical quantities in Figure 5.

according to their trends. The first part corresponds to a time during which inclination undergoes a rapid increase, reaching approximately 60° . Concurrently, the strength of B_z shows a rapid decrease, reaching approximately 500 G. These changes occur continuously during the first 30 minutes of the observation, coinciding with the formation of the LB. This indicates that the vertical magnetic fields of the sunspot umbra rapidly change to horizontal magnetic fields during the formation of the LB. The next part is a time at which a rapid decrease in inclination, with a rate of about -1.7° per minute, accompanied by an increase in B_z . We find that it is related to the dramatic changes that were observed in the internal structures of the photospheric LB, specifically, the bundle of filaments seen inside the LB rapidly disappeared and the granular structures began to appear along the LB. Thereafter, the convective motion was gradually predominant inside the LB, and in the latter half of the observation, two umbrae that had been divided were merged again, so that the LB began to disappear. It can be seen that the temporal changes of inclination and B_z observed during this final period proceed relatively slowly compared to the previous two evolutionary stages.

The temporal variations of B_h is also observed depending on the LB evolution, while the range of change is relatively smaller than others. Interestingly, we confirm that the strength of B_h is higher than that of B_z during the LB formation and filamentary LB but is weak during the granular LB. Our results indicate that the evolution of the LB is closely related to the changes of the magnetic field structures inside the sunspot.

3.3. Chromospheric Bright Jets

Temporal variations in magnetic field structures and sub-structural motion in the photosphere can directly influence the atmospheric activity above the LB. Figure 6 shows consecutive images obtained at varying wavelengths across from the line center to wings of the Ca II 854.2 nm and H α spectral lines, which were taken by FISS. These raster images demonstrate in detail the temporal variations in the chromospheric structure and activity following the evolutions of the LB. The chromospheric structure that stands out first in the images is fine-scale bright jets indicated by red arrows in Figure 6. These jets, which are approximately 2" in size, can be readily identified in the Ca II -0.5Å images. They occur intermittently and recurrently along the boundary between the LB and the host sunspot umbra.

We find from the figure that bright jets show characteristics varying with time. At the beginning of the observation, the bright jets mainly occurred along the leading edge of the LB where the filaments penetrate into the umbra, and the base of these jets was observed at the boundary between the LB and the host sunspot umbra as the enhanced

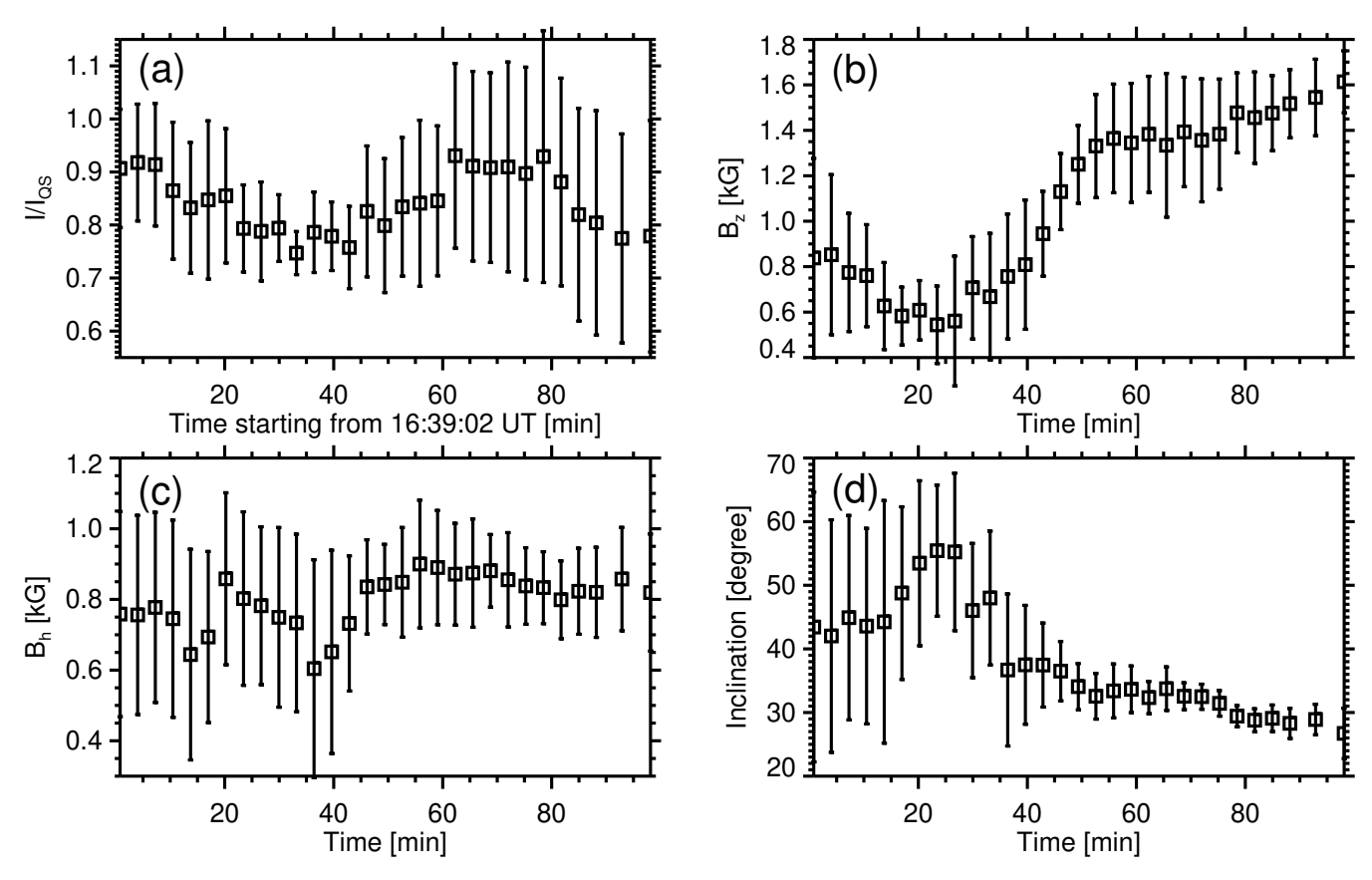


Figure 5. Temporal variations of (a) I/I_{QS} , (b) B_z , (c) B_h , and (d) inclination. The rectangle symbols represent the average values measured from several pixels along the LB. The error bars represent $\pm 1\sigma$ values resulting from the spatial distribution along the LB. Here, we set the observation time of 16:39:02 UT to t=0 min.

brightness. The jet's origin coincides with a region where the magnetic field topology is changing rapidly. After the LB is formed, the jets changed to the form of a fan-shaped jet as it expands along the LB. Afterward, the base of the jet slightly shifts backward along the LB, and the jet occurrence primarily concentrated around the midpoint of the LB. This evolution of a bright jet is consistent with the evolution of dark plasma ejections inside a filamentary LB previously reported by Lim et al. (2020). On the other hand, these jets are not well observed in the H α images. Instead, it can be observed that the base of the jets manifests as elongated brightening along the LB (see, H $\alpha \pm 0.7$ Å images).

Here, we noted that the bright jets are actively occurring for about 78 minutes following the start of our observation, but no further jets are ejected above the LB afterward, and the chromospheric structures remains relatively quiet. Here, we paid attention to the time of $t_{obs} \sim 78$ minutes. First, it is the timing when the strong bidirectional or unidirectional motion along the LB completely changes to the convective motion. The second thing is that prior to $t_{obs} \sim 78$ minutes, the internal structure of the LB seen in the photosphere undergoes a dramatic change, but after this time, it maintains a stable granular shapes which gradually begins to disappear. Of particular importance is the change in the internal magnetic field structure of the LB, which shows a rapid change before this time, but not afterwards. This suggests that the generation of the jets are closely related to the evolutionary stage of the LB, i.e., the temporal variation of the magnetic field of the LB within the sunspot umbra.

We conducted calculations of the vertical electric current density, J_z , around and inside the LB using the vector magnetic fields, B_x and B_y . Figure 7 shows three examples of J_z maps obtained at different times. The background of the figure was selected as the Ca II -0.5Å image, in which the bright jets can be well identified, and the J_z signals were represented by filled contours as reddish and bluish colors in each image. The white contour in the figure presents the boundary of the LB. We can see from the figure that enhanced currents patches are primarily observed along the boundary between the LB and the sunspot umbra. The location of strong currents within the LB is consistent with the previous findings reported by Shimizu (2011) and Lim et al. (2020). We find that the evolution of the enhanced

209

210

211

212

213

214

215

216

217

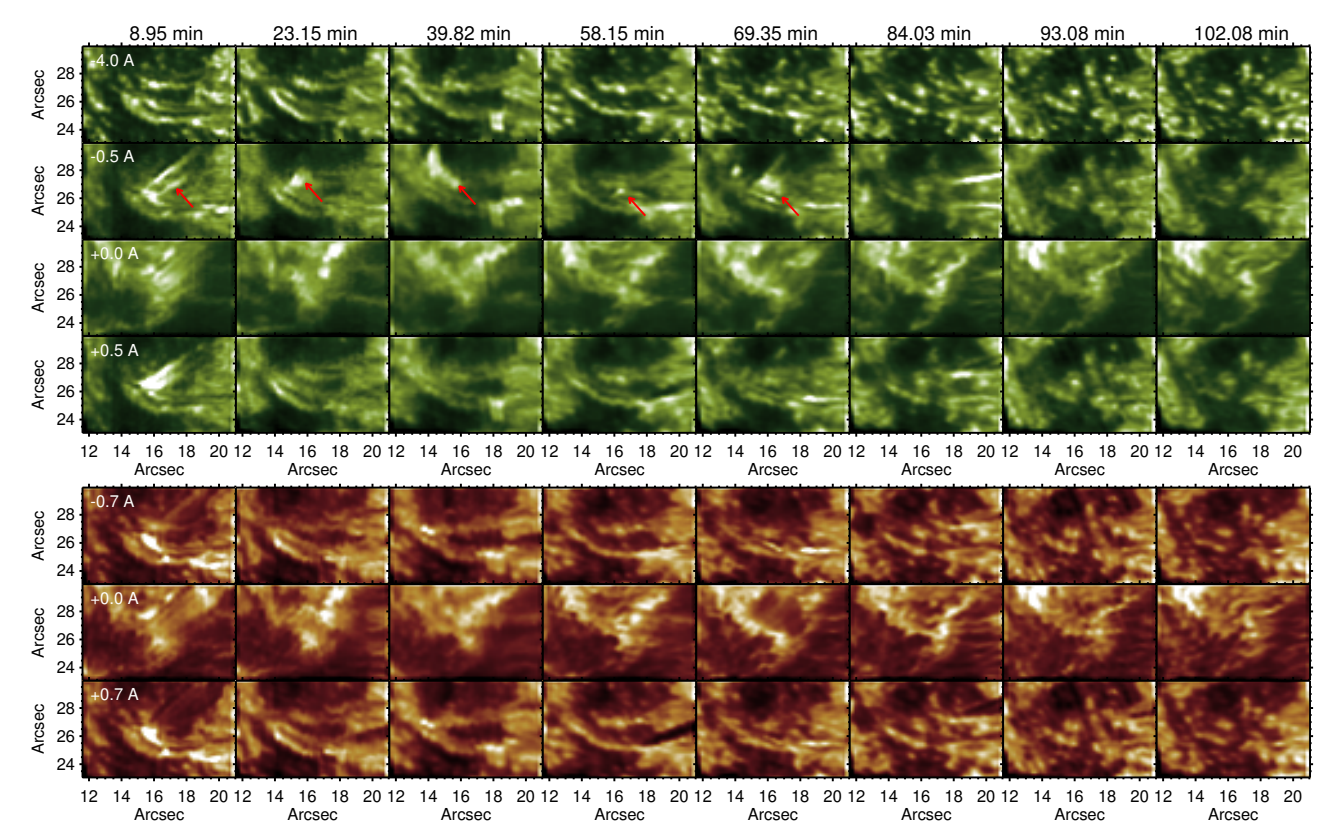


Figure 6. Consecutive chromospheric images obtained at varying wavelengths across from the line core to wings of the Ca II 854.2 nm (top) and H α (bottom) spectral lines, which were taken by FISS. The red arrows indicate bright jets occurring in the chromosphere.

currents are closely related to the occurrence of the bright jets. The strong currents were detected only during the period when the jets occurred intermittently, but did not appear thereafter. In particular, the location of the enhanced currents corresponded well with the base of the jets. It provides a critical observational evidence that the bright jets originate from magnetic reconnection that occurs at the boundary between the LB's new magnetic fields and the pre-existing magnetic fields of the ambient umbrae.

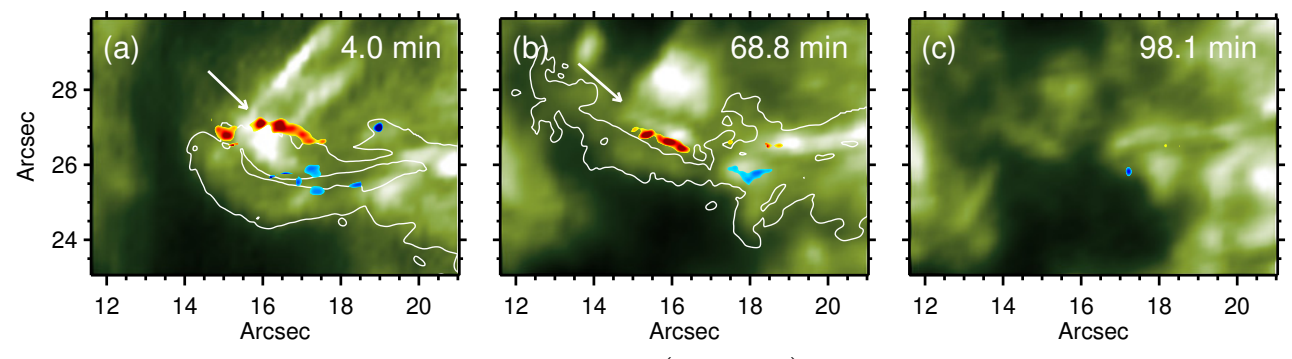


Figure 7. Maps of the vertical electric current density, $J_z = \frac{1}{\mu_0} \left(\frac{\partial B_y}{\partial x} - \frac{\partial B_x}{\partial y} \right)$, determined around the LB at the different time. Here, μ_0 is the magnetic permeability. The signals of J_z are saturated at $\pm 80 \text{ mA/m}^2$

4. DISCUSSION

We have reported on the short-term (several hours) evolution of a transient light bridge observed in the NOAA 12080 active region, as well as the changes of chromospheric phenomena above the host sunspot associated it by analyzing the imaging spectroscopic and spectropolarimetric data obtained from the 1.6 m GST/BBSO. Our observational data

are of important significance in that the evolution of the LB was observed within a short time of less than two hours, with high spatial and temporal resolutions. In particular, we find that the morphology, i.e., the internal structure, of the LB changes dramatically during its evolution, which enables a detailed exploration of not only the rapid changes in the internal physical properties of the sunspot and the LB, but also the temporal changes in the dynamical activity observed in the chromosphere. Our findings is important that it provides a comprehensive perspective to understand in detail not only the evolution of an LB itself with time, but also its impact on the neighboring regions, particularly changes in the chromospheric activity and magnetic energy of a sunspot.

The first thing that stands out in this study is that unlike the nature of a "normal" LB previously reported, there is a drastic change in the internal structure of the LB seen in the photosphere. According to the classification scheme of an LB (Korobova 1966; Muller 1979; Sobotka 1997), an LB can be generally categorized into "a filamentary LB" consisting of filament bundles and "a granular LB" with convective cell patterns, depending on the internal structure of an LB. Various previous LB studies show that most LBs have a single internal structure, such as a filamentary LB (Louis et al. 2008; Yang et al. 2019a; Hou et al. 2020) or a granular LB (Lagg et al. 2014; Song et al. 2017a), and they maintain a consistent morphology in the photosphere for a long time. Furthermore, the entire process of the LB evolution generally occurs over a long time. In particular, it has been reported that these differences in LB shapes mainly originate from differences in the structure of the magnetic field inside an LB and the process of LB formation (Katsukawa et al. 2007; Jurčák et al. 2006; Lagg et al. 2014; Okamoto & Sakurai 2018; Lim et al. 2020), and that LBs with different morphology can undergo different changes in physical properties during the evolution (Shimizu 2011; Griñón-Marín et al. 2021). Meanwhile, our findings show that these two shape differences are directly related to the evolutionary stage of the LB, i.e., rapid changes in the magnetic field and gas flow, inside the LB with time.

The LB of our interest was formed as a result of the strong intrusion of penumbral filaments with relatively horizontal fields into the vertical umbral field region. This is in good agreement with the results of previous studies that proposed the LB formation mechanism (Katsukawa et al. 2007; Louis et al. 2020). As the LB gradually formed, the magnetic non-potentiality inside the sunspot increases, and tangential discontinuity of the magnetic field appeared, especially around the local region where the magnetic field topology changes rapidly, i.e., the boundary region between the LB and umbrae. Indeed, we detected strong current density at this region (Shimizu et al. 2009; Lim et al. 2020), and distributed along the frontal boundary where the LB penetrates into the dark umbra in the early phase of the LB evolution. Afterward, the interior of the LB was gradually filled with filament bundles caused by the successive intrusion of penumbral filaments, and its morphology changes to a filamentary LB. From this point of time, the strong current mainly detected along the lateral-side of the LB. Interestingly, soon after, the filamentous structure disappeared and convective cells were observed to appear inside the LB. At this time, we saw that the magnetic field structure also changed rapidly in the vertical direction. As a result, its morphology changed from a filamentary LB to a granular LB.

The sudden disappearance of the filamentary structures inside a sunspot shows the observational manifestation that the magnetic relaxation process is occurring inside the sunspot. The formation of an LB may lead to the continuous buildup of free magnetic energy inside the sunspot until the fields become unstable. Once the magnetic field reaches a state of instability, it will seek to relax into a lower-energy state that is conserved the total magnetic flux and the magnetic helicity (Taylor 1974, 1986). We have observed the conversion of magnetic energy accumulated by the LB formation into kinetic and thermal energy as the magnetic relaxation process of a sunspot. The fine-scale bright jets, which are intermittently and recurrently observed in the chromosphere, are an important manifestation of this energy conversion. Our findings show that these jets occur mainly along the local region of magnetic discontinuity, i.e., strong current formed between the LB and the adjacent umbra, and this supports previous results that the origin of the observed jets above the LB is magnetic reconnection (Toriumi et al. 2015; Bharti et al. 2017; Tian et al. 2018). In particular, we find that the base of the jets appeared as an enhanced brightness along the strong current region, where is a counterpart region of the magnetic reconnection (Lim et al. 2020), and at the same time, the magnetic field inclination along the LB decreases rapidly. That is, it means that no additional horizontal magnetic field is supplied within the LB, and the LB magnetic field continuously changes into a vertical magnetic field. This process of horizontal field removal causes the weakening of the LB fields and breaks the balance between umbral fields and surrounding LB fields, causing the LB to fragment and start to turn into umbral dots.

Note that we observed in detail the magnetic relaxation process within a sunspot. The magnetic system of the sunspot initially in equilibrium became disturbed by the formation of the transient LB of several hour lifetime and then returned to a stable state again. This kind of relaxation process may be occurring during the evolution and

activity of the LBs of several day lifetime as well. Thus our results will contribute to the comprehensive understanding 270 of the evolution of LBs, and their relationship with the sunspot system and the associated chromospheric activity in 271 general. 272

This work was supported by the Korea Astronomy and Space Science Institute under the R&D program of the 273 Korean government (MSIT) (No. 2023-1-850-04, Development of a solar coronagraph on ISS). BBSO operation is 274 supported by US NSF AGS-2309939 and AGS-1821294 grants and New Jersey Institute of Technology. GST operation 275 is partly supported by the Korea Astronomy and Space Science Institute and the Seoul National University. YK was 276 supported by JSPS KAKENHI Grant Number JP23H01220. V.Y. acknowledges support from NASA 80NSSC20K0025, 277 80NSSC20K1282, and 80NSSC21K1671 grants, and NSF AGS 2309939, 2300341, and AST 2108235, 2114201 grants. 278

REFERENCES

334

- Berger, T. E. & Berdyugina, S. V. 2003, ApJL, 589, L117. 279 doi:10.1086/376494 280 Bharti, L., Solanki, S. K., & Hirzberger, J. 2017, A&A, 597, 281 A127. doi:10.1051/0004-6361/201629656 282 Cao, W., Gorceix, N., Coulter, R., et al. 2010, 283 Astronomische Nachrichten, 331, 636. 284 doi:10.1002/asna.201011390 285 Cao, W., Goode, P. R., Ahn, K., et al. 2012, Second 286 ATST-EAST Meeting: Magnetic Fields from the 287 Photosphere to the Corona., 463, 291 288 Chae, J. & Sakurai, T. 2008, ApJ, 689, 593. 289 doi:10.1086/592761 290 Chae, J., Park, H.-M., Ahn, K., et al. 2013, SoPh, 288, 1. doi:10.1007/s11207-012-0147-x 292 Griñón-Marín, A. B., Pastor Yabar, A., Centeno, R., et al. 293
- 153. 296 Hou, Y. J., Li, T., Zhong, S. H., et al. 2020, A&A, 642, 297 A44. doi:10.1051/0004-6361/202038668

2021, A&A, 647, A148. doi:10.1051/0004-6361/202039847

Hale, G, E., Ellerman, F, Nicholson, S, B. 1919, ApJ, 49,

- Jurčák, J., Martínez Pillet, V., & Sobotka, M. 2006, A&A, 299 453, 1079. doi:10.1051/0004-6361:20054471 300
- Katsukawa, Y., Yokoyama, T., Berger, T. E., et al. 2007, 301 PASJ, 59, S577. doi:10.1093/pasj/59.sp3.S577
- Korobova, Z. B. 1966, AZh, 43, 480 303

294

295

298

310

314

- Lagg, A., Solanki, S. K., van Noort, M., et al. 2014, A&A, 304 568, A60. doi:10.1051/0004-6361/201424071 305
- Landi Degl'Innocenti, E. 1992, Solar Observations: 306
- Techniques and Interpretation, 71 307
- Leka, K. D. 1997, ApJ, 484, 900. doi:10.1086/304363 308
- Lim, E.-K., Yang, H., Yurchyshyn, V., et al. 2020, ApJ, 309
 - 904, 84. doi:10.3847/1538-4357/abc1e0
- Louis, R. E., Bayanna, A. R., Mathew, S. K., et al. 2008, 311 SoPh, 252, 43. doi:10.1007/s11207-008-9247-z 312
- Louis, R. E., Beck, C., & Ichimoto, K. 2014, A&A, 567, 313 A96. doi:10.1051/0004-6361/201423756

- Louis, R. E., Bellot Rubio, L. R., de la Cruz Rodríguez, J., et al. 2015, A&A, 584, A1.
- doi:10.1051/0004-6361/201526854 317
- Louis, R. E., Beck, C., & Choudhary, D. P. 2020, ApJ, 905, 153. doi:10.3847/1538-4357/abc618 319
- Moon, Y.-J., Wang, H., Spirock, T. J., et al. 2003, SoPh, 320 217, 79. doi:10.1023/A:1027365413021 321
- Muller, R. 1979, SoPh, 61, 297. doi:10.1007/BF00150414 322
- Okamoto, T. J. & Sakurai, T. 2018, ApJL, 852, L16. 323
- doi:10.3847/2041-8213/aaa3d8 324
- Pesnell, W. D., Thompson, B. J., & Chamberlin, P. C. 325 2012, SoPh, 275, 3. doi:10.1007/s11207-011-9841-3 326
- Schou, J., Scherrer, P. H., Bush, R. I., et al. 2012, SoPh, 327 275, 229. doi:10.1007/s11207-011-9842-2 328
- Schüssler, M. & Vögler, A. 2006, ApJL, 641, L73. 329 doi:10.1086/503772 330
- Shimizu, T., Katsukawa, Y., Kubo, M., et al. 2009, ApJL, 331 696, L66. doi:10.1088/0004-637X/696/1/L66
- Shimizu, T. 2011, ApJ, 738, 83.
 - doi:10.1088/0004-637X/738/1/83
- Shumko, S., Gorceix, N., Choi, S., et al. 2014, Proc. SPIE, 9148, 914835. doi:10.1117/12.2056731 336
- Sobotka, M., Bonet, J. A., & Vazquez, M. 1994, ApJ, 426, 337 404. doi:10.1086/174076 338
- Sobotka, M. 1997, 1st Advances in Solar Physics 339
- Euroconference. Advances in Physics of Sunspots, 118, 340 341
- Song, D., Chae, J., Park, S., et al. 2015, ApJL, 810, L16. 342 doi:10.1088/2041-8205/810/2/L16 343
- Song, D., Chae, J., Yurchyshyn, V., et al. 2017a, ApJ, 835, 344 240. doi:10.3847/1538-4357/835/2/240 345
- Song, D., Chae, J., Kwak, H., et al. 2017b, ApJL, 850, L33. 346 doi:10.3847/2041-8213/aa9a36 347
- Taylor, J. B. 1974, Physical Review Letters, 33, 2239.
- doi:10.1103/PhysRevLett.33.1139
- Taylor, J. B. 1986, Reviews of Modern Physics, 58, 741. 350 doi:10.1103/RevModPhys.58.741

- 352 Tian, H., Yurchyshyn, V., Peter, H., et al. 2018, ApJ, 854,
- 92. doi:10.3847/1538-4357/aaa89d
- ³⁵⁴ Toriumi, S., Cheung, M. C. M., & Katsukawa, Y. 2015,
- 355 ApJ, 811, 138. doi:10.1088/0004-637X/811/2/138
- ³⁵⁶ Vazquez, M. 1973, SoPh, 31, 377. doi:10.1007/BF00152814
- Wöger, F., von der Lühe, O., & Reardon, K. 2008, A&A,
- $488,\ 375.\ doi:10.1051/0004\text{-}6361\text{:}200809894$
- ³⁵⁹ Yang, H., Lim, E.-K., Iijima, H., et al. 2019a, ApJ, 882,
- 360 175. doi:10.3847/1538-4357/ab36b7
- ³⁶¹ Yang, X., Yurchyshyn, V., Ahn, K., et al. 2019b, ApJ, 886,
- 64. doi:10.3847/1538-4357/ab4a7d
- ³⁶³ Zhang, J., Tian, H., He, J., et al. 2017, ApJ, 838, 2.
- doi:10.3847/1538-4357/aa63e8